6th International Conference on
Bulk Materials Storage, Handling and Transportation
Wollongong NSW, Australia, 28-30 September 1998

Discrete Inverse Wavelets Transform Analysis For Spiral Flow Pneumatic Conveying

Masahiro TAKEI[1], Hui LI[2], Yao-Hua ZHAO[3], Mitsuaki OCHI[1]
Yoshifuru SAITO[4], Kiyoshi HORII[5] and Hiroshi NISHIMURA[6]

1 Department of Mechanical Engineering, Nihon University, Tokyo Japan
2 Kagoshima University, Kagoshima Japan,
3 University of Tokyo, Tokyo Japan
4 Hosei University, Tokyo Japan,
5 Shirayuri Women's College, Tokyo Japan
6 Amano Corporation, Shizuoka Japan

Summary Two dimensional directions of regular particle movements in two phase spiral flow have been clearly extracted after reducing irregular particle movements by means of discrete wavelets transform and its multiresolution analysis. The method is composed of three steps. Firstly, the two dimensional particle velocities at a cross section are transformed to the wavelets spectrum by the discrete wavelets transform. Secondly, the wavelets spectrum data are inversely transformed to each multiresolution level by means of the discrete inverse wavelets transform. Finally, after some multiresolution levels including the irregular data are reduced, the other level results in extracting the regular data that indicate two dimensional directions of the regular particle movements.

1 INTRODUCTION

A high performance pneumatic transportation system using spiral flow which has a steep axial velocity profile and swirling motion with large free vortex region was preliminarily developed[1]. The rotating particles in this transportation system tend not to touch the pipe inner wall because the particles obtain high centripetal force from the spiral flow with the steep axial velocity distribution. The system is useful for the pneumatic transportation of fragile and sticky materials in chemical and food industries due to avoiding material breaking and sticking to the pipe inner wall. It is important to make clear the relation between the air velocity distribution and the particle velocity distribution in the two phase spiral flow to improve the system performance. The orderly analysis to estimate the particles movement from the air velocity distributions has been used in order to analyze the relation[2]. Nowadays, inverse problems have been treated in the other fields such as material engineering[3]. We have applied the idea of the inverse problem to analyzing the two phase spiral flow to estimate the air velocity distributions from the particles movement. The inverse analysis has two aspects, which are the extraction of the regular particle movements, and the estimate of the air velocities from the extracted particle velocities. This paper focuses on the extraction of the regular particle movements in the spiral flow. The originality of this paper lies in applying discrete wavelets transform and its multiresolution analysis to the two dimensional vector data in the two phase spiral flow in order to achieve the inverse problem.

Wavelets transform[4] is roughly classified with two types, which are continuous wavelets transform and discrete wavelets transform. The continuous wavelets transform has been generally used for time frequency analysis in vibration wave. The analysis enables to analyze simultaneously time and frequency and to extract peculiar points. Li classified eddy frequency passing in jet flow[5]. On the other hand, the discrete wavelets transform has been mainly used for picture image processing. The analysis enables compression of picture image data and removal of peculiar points from the picture image data. Saito applied this idea to analyzing the electromagnetic wave[6].

In this paper, after describing the theory of discrete wavelets transform, the velocities of rotating particles on a cross section in the two phase spiral flow are measured. Next, the directions of the regular particle movements are extracted from the velocities after reducing the irregular particle movements by means of discrete wavelets transform and its multiresolution analysis.

2 THEORY OF DISCRETE WAVELETS TRANSFORM

The continuous wavelets transform $WT(b,a)$ of a real square integrable function $f(x)$ is defined as[4)]

$$WT(b,a)=\frac{1}{\sqrt{|a|}}\int_{-\infty}^{\infty} f(x)\overline{\varphi\left(\frac{x-b}{a}\right)}dx \qquad \text{——(1)}$$

Where, $f(x)$ is a target function with regard to one dimensional space x such as vibration data and image data, a is a scale variable, b is a location variable, and $\phi(x)$ is a real integrable analyzing wavelets with zero at large x

and at small x. The function $f(x) \in L^2(R)$ at a location b and a scale a. $L^2(R)$ denotes Hilbert space. $\phi((x-b)/a)$ is a function to scale $\phi(x)$ by a times in x direction and to translate it by b. $\phi(x)$ is satisfied with the next admissible condition,

$$\int_{-\infty}^{\infty} \varphi(x)dx = 0 \qquad \text{——(2)}$$

From Eq. (1), after the scale variable a and the location variable b change to the discrete values; $a = 2^{-j}$ and $b = 2^{-j}k$ (j and k are integers), the discrete wavelets transform is expressed by

$$WT_k^{(j)} = 2^{\frac{j}{2}} \int_{-\infty}^{\infty} f(x)\overline{\varphi(2^j x - k)dx} \qquad \text{——(3)}$$

$\phi(2^j x - k)$ can be an orthonormal function when $\phi(x)$ is a special function. From Eq. (3), the discrete inverse wavelets transform is expressed by

$$f(x) = \sum_{j=-\infty}^{\infty} \sum_{k=-\infty}^{\infty} WT_k^{(j)} \varphi(2^j x - k) \qquad \text{——(4)}$$

Eq. (3) becomes simple matrix operations when the elements of $f(x)$ is composed of discrete values. When the sampling number in terms of $f(x)$ in x direction is n (n is a second exponent value), a matrix $\mathbf{X}$ that indicates $f(x)$ in Eq. (3) has the sampling data. The wavelets spectrum matrix $\mathbf{S}$ that indicates $WT_k^{(j)}$ in Eq. (3) is obtained from

$$\mathbf{S} = \mathbf{W_n} \cdot \mathbf{X} \qquad \text{——(5)}$$

Where, $\mathbf{W_n}$ is discrete analyzing wavelets matrix that indicates $\phi(2^j x - k)$ in Eq. (3). In this analysis, sixth dimensional Daubechies function is used as the analyzing wavelets. The analyzing wavelets is an orthonormal function. The analyzing wavelets matrix $\mathbf{W_n}$ is acquired by a cascade algorithm on the basis of a scaling function matrix $\mathbf{C}$. The scaling function is shown in Eq. (6).

$$\mathbf{C} = \begin{pmatrix}
c_0 & c_1 & c_2 & c_3 & c_4 & c_5 & 0 & 0 & \cdot & 0 & 0 & 0 & 0 & 0 & 0 & 0 & 0 \\
c_5 & -c_4 & c_3 & -c_2 & c_1 & -c_0 & 0 & 0 & \cdot & 0 & 0 & 0 & 0 & 0 & 0 & 0 & 0 \\
0 & 0 & c_0 & c_1 & c_2 & c_3 & c_4 & c_5 & \cdot & 0 & 0 & 0 & 0 & 0 & 0 & 0 & 0 \\
0 & 0 & c_5 & -c_4 & c_3 & -c_2 & c_1 & -c_0 & \cdot & 0 & 0 & 0 & 0 & 0 & 0 & 0 & 0 \\
\cdot & \cdot & \cdot & \cdot & \cdot & \cdot & \cdot & \cdot & \cdot & \cdot & \cdot & \cdot & \cdot & \cdot & \cdot & \cdot & \cdot \\
c_4 & c_5 & 0 & 0 & 0 & 0 & 0 & 0 & \cdot & 0 & 0 & 0 & 0 & c_0 & c_1 & c_2 & c_3 \\
c_1 & -c_0 & 0 & 0 & 0 & 0 & 0 & 0 & \cdot & 0 & 0 & 0 & 0 & c_5 & -c_4 & c_3 & -c_2 \\
c_2 & c_3 & c_4 & c_5 & 0 & 0 & 0 & 0 & \cdot & 0 & 0 & 0 & 0 & 0 & 0 & c_0 & c_1 \\
c_3 & -c_2 & c_1 & -c_0 & 0 & 0 & 0 & 0 & \cdot & 0 & 0 & 0 & 0 & 0 & 0 & c_5 & -c_4
\end{pmatrix} \qquad \text{——(6)}$$

$$\left.\begin{aligned}
c_0 &= \frac{1}{16\sqrt{2}}\left(1+\sqrt{10}+\sqrt{5+2\sqrt{10}}\right) \quad c_1 = \frac{1}{16\sqrt{2}}\left(5+\sqrt{10}+3\sqrt{5+2\sqrt{10}}\right) \quad c_2 = \frac{1}{8\sqrt{2}}\left(5-\sqrt{10}+\sqrt{5+2\sqrt{10}}\right) \\
c_3 &= \frac{1}{8\sqrt{2}}\left(5-\sqrt{10}-\sqrt{5+2\sqrt{10}}\right) \quad c_4 = \frac{1}{16\sqrt{2}}\left(5+\sqrt{10}-3\sqrt{5+2\sqrt{10}}\right) \quad c_5 = \frac{1}{16\sqrt{2}}\left(1+\sqrt{10}-\sqrt{5+2\sqrt{10}}\right)
\end{aligned}\right\} \qquad \text{——(7)}$$

$$c_5 - c_4 + c_3 - c_2 + c_1 - c_0 = 0 \qquad \text{——(8)} \qquad 0\,c_5 - 1\,c_4 + 2\,c_3 - 3c_2 + 4\,c_1 - 5\,c_0 = 0 \qquad \text{——(9)}$$

Where, $\mathbf{C^T \cdot C = I}$, $\mathbf{I}$ is a unit matrix and $\mathbf{C^T}$ is a transpose matrix of $\mathbf{C}$. In Eq. (6), the first line shows a transform to get the mean values to put the weights from c_0 to c_5 on the input data. The second line shows a transform to get the difference values to put the weights from c_0 to c_5 on the input data. The third line shows a transform to translate the first line by two steps in x direction. The fourth line is a transform to do the second line by two steps. Eqs. (8) and (9) show the transformed values are zero when the input data are constant or simply increased. To explain easily the process to acquire the analyzing wavelets matrix $\mathbf{W_n}$ from $\mathbf{C}$, the matrix $\mathbf{X}$ is defined as one dimensional 16 elements,

$$\mathbf{X} = [x_1\, x_2\, x_3\, x_4\, x_5\, x_6\, x_7\, x_8\, x_9\, x_{10}\, x_{11}\, x_{12}\, x_{13}\, x_{14}\, x_{15}\, x_{16}]^T \qquad \text{——(10)}$$

From Eqs. (6) and (10), the transformed matrix $\mathbf{X'}$ is

$$\mathbf{X'} = \mathbf{C_{16}X} = [s_1\, d_1\, s_2\, d_2\, s_3\, d_3\, s_4\, d_4\, s_5\, d_5\, s_6\, d_6\, s_7\, d_7\, s_8\, d_8\,]^T \qquad \text{——(11)}$$

Where, $\mathbf{C_{16}}$ is a 16X16 matrix of $\mathbf{C}$. The element s indicates the mean value and the element d indicates the difference value. The elements in the matrix $\mathbf{X'}$ are replaced by a matrix $\mathbf{P_{16}}$.

$$\mathbf{P_{16}X'} = \mathbf{P_{16}\,C_{16}X} = [s_1\, s_2\, s_3\, s_4\, s_5\, s_6\, s_7\, s_8\, d_1\, d_2\, d_3\, d_4\, d_5\, d_6\, d_7\, d_8\,]^T \qquad \text{——(12)}$$

Where, $\mathbf{P_{16}}$ is a 16X16 matrix such as

$$\mathbf{P}_{16}=\begin{pmatrix}
1&0&0&0&0&0&0&0&0&0&0&0&0&0&0&0\\
0&0&1&0&0&0&0&0&0&0&0&0&0&0&0&0\\
0&0&0&0&1&0&0&0&0&0&0&0&0&0&0&0\\
0&0&0&0&0&0&1&0&0&0&0&0&0&0&0&0\\
0&0&0&0&0&0&0&0&1&0&0&0&0&0&0&0\\
0&0&0&0&0&0&0&0&0&0&1&0&0&0&0&0\\
0&0&0&0&0&0&0&0&0&0&0&0&1&0&0&0\\
0&0&0&0&0&0&0&0&0&0&0&0&0&0&1&0\\
0&1&0&0&0&0&0&0&0&0&0&0&0&0&0&0\\
0&0&0&1&0&0&0&0&0&0&0&0&0&0&0&0\\
0&0&0&0&0&1&0&0&0&0&0&0&0&0&0&0\\
0&0&0&0&0&0&0&1&0&0&0&0&0&0&0&0\\
0&0&0&0&0&0&0&0&0&1&0&0&0&0&0&0\\
0&0&0&0&0&0&0&0&0&0&0&1&0&0&0&0\\
0&0&0&0&0&0&0&0&0&0&0&0&0&1&0&0\\
0&0&0&0&0&0&0&0&0&0&0&0&0&0&0&1
\end{pmatrix} \quad \text{——(13)}$$

Moreover, from Eq. (11), the transform is carried out by **C** and **P**,

$$\mathbf{S}=\mathbf{W}^{(2)}\mathbf{X}=[S_1\ S_2\ S_3\ S_4\ D_1\ D_2\ D_3\ D_4\ d_1\ d_2\ d_3\ d_4\ d_5\ d_6\ d_7\ d_8]^T \quad \text{——(14)}$$

Where,

$$\mathbf{W}^{(2)}=(\mathbf{P}_{16}\text{'}\mathbf{C}\text{'}_{16})(\mathbf{P}_{16}\mathbf{C}_{16}) \quad \text{——(15)} \qquad \mathbf{P}_{16}\text{'}=\begin{bmatrix}\mathbf{P}_8&\mathbf{0}\\ \mathbf{0}&\mathbf{I}_8\end{bmatrix}\quad \mathbf{C}_{16}\text{'}=\begin{bmatrix}\mathbf{C}_8&\mathbf{0}\\ \mathbf{0}&\mathbf{I}_8\end{bmatrix} \quad \text{——(16)}$$

$\mathbf{W}^{(2)}$ is a analyzing wavelets matrix that is $\mathbf{W}_n$ in Eq. (5). The wavelets spectrum **S** in Eq. (5) is $\mathbf{W}^{(2)}\mathbf{X}$ in Eq. (14). In Eq. (14), S_1 indicates the mean value from s_1 to s_6 in Eq. (12). S_2 indicates the mean value from s_3 to s_8 that translate by two steps. D_1 indicates the difference value from s_1 to s_6. From Eq. (14), the input data are transformed to the mean value and difference value with valuable resolution levels by the discrete wavelets transform. The input data in the space are divided into the range from high frequency to low frequency.

From Eqs. (5) and (14), the inverse wavelets transform is,

$$\mathbf{X}=\mathbf{W}_n{}^T\mathbf{S}=[\mathbf{W}^{(2)}]^T\mathbf{S} \quad \text{——(17)}$$

$$[\mathbf{W}^{(2)}]^T=[(\mathbf{P}_{16}\text{'}\ \mathbf{C}_{16}\text{'})(\mathbf{P}_{16}\mathbf{C}_{16})]^T=\mathbf{C}_{16}{}^T\mathbf{P}_{16}{}^T(\mathbf{C}_{16}\text{'})^T(\mathbf{P}_{16}\text{'})\mathbf{T} \quad \text{——(18)}$$

In Eq. (5), one dimensional space is replaced with two dimensional space in x and y directions. When the sampling number in x direction is n and that in y direction is m (n and m are second exponent values), a matrix **H** (nXm) has the sampling data. The two dimensional wavelets spectrum **S** is obtained from

$$\mathbf{S}=\mathbf{W}_n\cdot\mathbf{H}\cdot\mathbf{W}_m{}^T \quad \text{——(19)}$$

Where, $\mathbf{W}_m{}^T$ is a transpose matrix of $\mathbf{W}_n$.

In this analysis, because the velocity data located at each grid are vector data, x component and y component are calculated separately in Eq. (19). The two dimensional wavelets spectrum of x component of the vector data $\mathbf{S}_x$ and that of y component $\mathbf{S}_y$ are obtained from

$$\mathbf{S}_x=\mathbf{W}_n\cdot\mathbf{H}_x\cdot\mathbf{W}_m{}^T \qquad \mathbf{S}_y=\mathbf{W}_n\cdot\mathbf{H}_y\cdot\mathbf{W}_m{}^T \quad \text{——(20)}$$

Where, $\mathbf{H}_x$ and $\mathbf{H}_y$ are nXm matrixes to show x and y components of the velocity vector data. The elements of the matrix show the velocities on the grid of the particle position. From Eq. (20), the discrete inverse wavelets transform is expressed by

$$\mathbf{H}_x=\mathbf{W}_n{}^T\cdot\mathbf{S}_x\cdot\mathbf{W}_m \qquad \mathbf{H}_y=\mathbf{W}_n{}^T\cdot\mathbf{S}_y\cdot\mathbf{W}_m \quad \text{——(21)}$$

In this analysis, n =16 and m =16.

3 EXPERIMENTS

3.1 Nozzle to Produce Spiral Flow & its Characteristics

The nozzle to produce the spiral flow is designed with an annular slit connecting to a conical cylinder as shown in Fig. 1[7]. Pressurized air is forced through the sides of the device into the buffer area, and then through the annular slit into a vertical pipe entrance. The suction force is generated at the back of the nozzle by Coanda effect. The annular jet, passing through the conical cylinder, develops a spiral structure with a steeper axial velocity and an azimuthal velocity distributions, even if it is not applied tangentially[8]. Particles at the back of the nozzle are sucked into the nozzle to be issued to the pipe as rotating. The characteristics of the single phase spiral flow has been reported[9]. According to the paper, the divergence angle of the spiral flow issued from the nozzle outlet is reduced 45 %, from 14.3 degrees to 7.8 degrees as compared with typical turbulence flow. These results clearly indicates the focusing characteristic and the high stability of the spiral flow. The particles in the two phase spiral flow obtain high centripetal force.

3.2 Experimental Equipment, Method & Conditions

The experimental equipment consisted of a vertical acrylic pipe, the nozzle to produce the spiral flow, a CCD camera and an air compressor as shown in Fig. 2. The inside diameter of the vertical pipe is 41.0 mm and the height of the pipe is 1.5 m. The CCD camera to focus on a two dimensional cross section of the vertical pipe is set up at the top of the vertical pipe to record the particle trajectories. With the experimental equipment, the movement of the particles (styrofoam balls) in the spiral flow on a two dimensional cross section are observed. The balls rotate inside the cross section of the vertical pipe when the gravity on the ball is balanced by the drag force due to the upward velocity component of the spiral air flow. The styrofoam balls are sucked from the intake part of the nozzle. The diameter of the balls is 6 mm and the particle density is 700 kg/m^3. The air flow rate is 5.5 X 10^{-3} m^3/s. The mean velocity of the air flow in the vertical pipe calculated from the flow rate is 4.2 m/s. The Reynolds number calculated from the velocity is about 5700 .

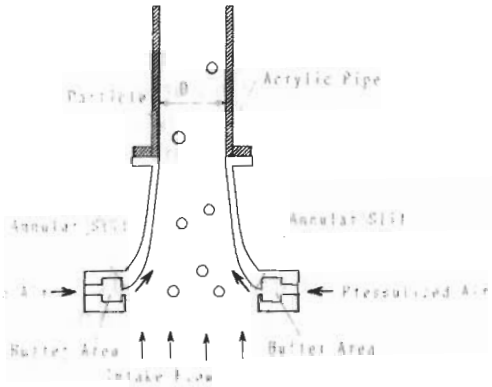

Fig. 1 Spiral flow nozzle

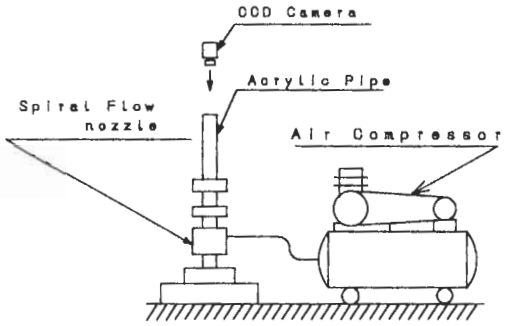

Fig. 2 Experimental equipment

3.3 Experimental Results

As an initial experiment to clarify the ball movement in the two phase spiral flow compared to that in a typical turbulence flow, several styrofoam balls movements were observed from the side of the vertical pipe on the above experimental conditions. The balls in the spiral flow rotated on a cross section of the vertical pipe at 0.8 m height from the outlet of the nozzle without touching the pipe inner wall as shown in Fig. 3 (a). The flow direction in the figure is upward and the gravity force on the balls is balanced by the drag force. If the flow rate increases, the balls move up as a rotating spiral. On the other hand, the balls in a typical turbulence flow move randomly upward and downward colliding with the pipe inner wall as shown in Fig. 3 (b).

Next, many styrofoam ball movements in the spiral flow are observed from the top of the pipe for the same experimental conditions. The two dimensional velocity vector of the balls on a cross section are acquired from the recorded particles trajectories. An example of the velocity vector is shown in Fig. 4. In this figure, the positions of the vector data are shown on a 16X16 grid to simplify further analysis. The length of the vector indicates the magnitude of the particle velocity, and the direction of the vector indicates the two dimensional direction of the particle movement. From the figure, the balls rotate counter-clockwise. Some particles move irregularly due to interference and collisions with other balls. For example, a particle located at (10, 4) moves in the y direction; however, other particles around this particle have x and y component velocities.

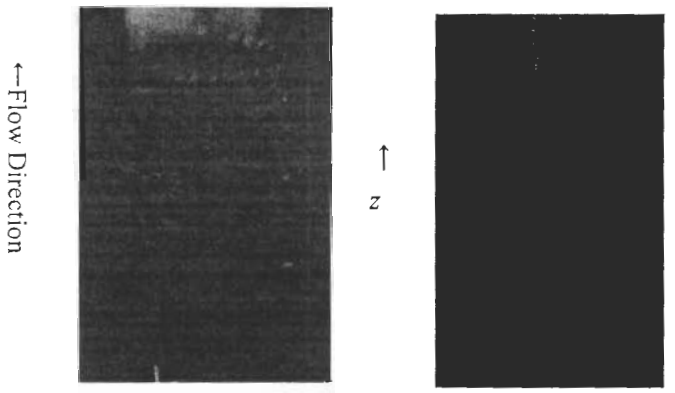

(a) Particles in spiral flow (b) Particles in turbulence flow

Fig. 3 Particle movements in spiral flow and turbulence flow

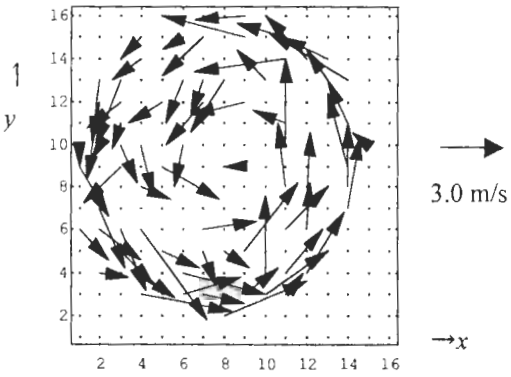

Fig. 4 Two dimensional velocity vector of particles in spiral flow

4 ANALYSIS AND DISCUSSION

4.1 Assumptions for Analysis

The following assumptions and prior conditions are set up. (1) The air velocity V_a is given by

$$V_a = V_p + V'(d, Re, \nu_d/\nu_p) \qquad \text{——(22)}$$

Where, V_p is particle velocity and V' is additional velocity on a particle. When $d/L(Re) < 1$ and $\nu_d/\nu_p = 1$, $V' = 0$. L is characteristic eddy length, d is particle diameter, Re is Reynolds number, ν_a is air viscosity and ν_p is viscosity of particle surface. In this analysis, the particles does not follow the air movement as $V' \neq 0$. (2)The instantaneous particle velocity distribution in Fig. 4 is considered. (3)Only a two-dimensional horizontal cross section of the pipe is considered. The velocity component in the z direction is ignored. (4)The velocity at a mesh point without any particles is assumed to be zero.

4.2 Analysis Method

This analysis consists of three steps. Firstly, the two dimensional vector data of the particles velocities in Fig. 4, $\mathbf{H}_x$ and $\mathbf{H}_y$, are respectively transformed to the wavelets spectrum $\mathbf{S}_x$ and $\mathbf{S}_y$ by means of the discrete wavelets transform in x and y components in Eq. (20).

Next, the multiresolution analysis can be carried out because the wavelets transform is an orthonormal transform, that is, each part of the spectrum is inversely transformed to three multiresolution levels by means of the discrete inverse wavelets transform. From Eq. (17), to explain easily, the multiresolution analysis about one dimensional data is,

$$\mathbf{X} = [\mathbf{W}^{(2)}]^{\mathrm{T}}\mathbf{S} = [\mathbf{W}^{(2)}]^{\mathrm{T}}\mathbf{S}_1 + [\mathbf{W}^{(2)}]^{\mathrm{T}}\mathbf{S}_2 + [\mathbf{W}^{(2)}]^{\mathrm{T}}\mathbf{S}_3 \qquad \text{——(23)}$$

Where,

$$\mathbf{S}_1 = [S_1\ S_2\ S_3\ S_4\ 0\ 0\ 0\ 0\ 0\ 0\ 0\ 0\ 0\ 0\ 0\ 0]^T \qquad \mathbf{S}_2 = [0\ 0\ 0\ 0\ D_1\ D_2\ D_3\ D_4\ 0\ 0\ 0\ 0\ 0\ 0\ 0\ 0]^T$$
$$\mathbf{S}_3 = [0\ 0\ 0\ 0\ 0\ 0\ 0\ 0\ d_1\ d_2\ d_3\ d_4\ d_5\ d_6\ d_7\ d_8]^T \qquad \text{——(24)}$$

In Eq. (23), the first term is Level 1 which includes the lower frequency of input data, the second term is Level 2 which includes the middle frequency, and the third term is Level 3 which includes the higher frequency. Namely, Level 1 shows the mean particle movement except for the random particle movement. On the other hand, Level 3 shows the random particle movement except for the mean particle movement.

Finally, each level is considered if it has irregular data. Then, after some multiresolution levels including the irregular data are reduced, the other level results in extracting the regular data that indicate two dimensional directions of the regular particle movements.

4.3 Analysis Results & Discussion

Figs. 5 (a) and (b) show the wavelets spectrum of x and y components of the particle velocities by means of the discrete wavelets transform in Eq. (20). In these figures, the whiter parts at each grid show the larger transformed values, the darker parts show the lower transformed values. Each part is drawn by gray scale with ten patterns. In this analysis, the transformed data are separated from the low frequency level to the high frequency level by the discrete wavelets transform. In Figs 5 (a) and (b), from Eqs.(23) and (24), the low frequency level concentrates on the inside of 4X4 parts (from S_1 to S_4 in Eq. (24)) in the spectrum. The middle frequency level collects inside 8X8 parts except 4X4 parts (from D_1 to D_4 in Eq. (24)) in the spectrum. The high frequency level collects inside 16X16 parts except 8X8 parts (from d_1 to d_8 in Eq. (24)) in the spectrum.

Fig. 6 shows the results of the multiresolution analysis from transforming inversely each part of the wavelets spectrum in Fig. 5. Fig. 6 (a) shows Level 1 which indicates the mean direction of the particle movement with low frequency level. The direction indicates swirling motion on the whole. Fig. 6 (b) is Level 2, which has the middle random vector. Fig. 6(c) is Level 3, which shows the large random vector with high level frequency.

From this multiresolution, the spectrum can be divided from low frequency level to high frequency level. Adding from level 1 to level 3, the original velocity vector in Fig. 4 is completely recovered because the discrete wavelet transform is an orthonormal. From Fig. 6(a), the regular particles movements are clearly obtained.

Additionally, adding from Level 1 to Level 2 results in Fig. 7 after reducing Level 3. Fig. 6(a) shows the regular particle movements more clearly than Fig. 7.

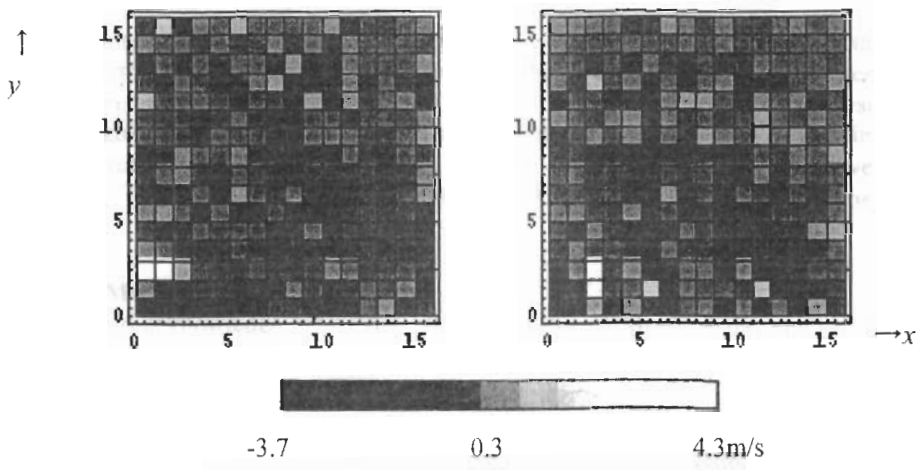

(a) Spectrum in x component (b)Spectrum in y component

Fig. 5 Wavelets spectrum from particle velocity

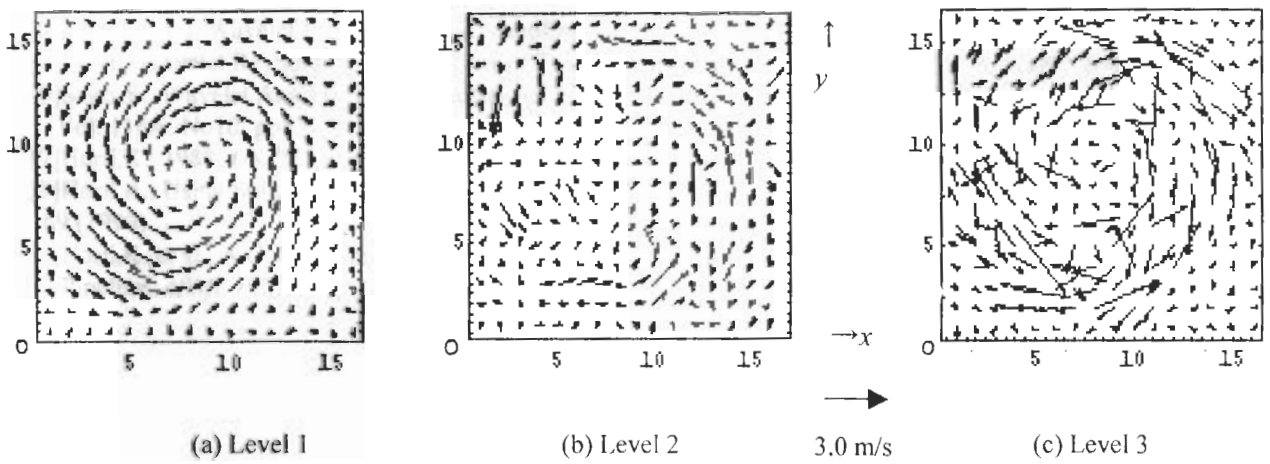

(a) Level 1 (b) Level 2 (c) Level 3

Fig. 6 Multiresolution analysis

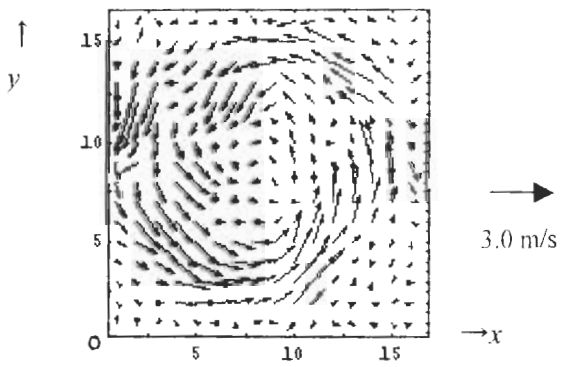

Fig. 7 Adding Level 1 and Level 2

5 CONCLUSIONS

Two dimensional directions of regular particle movements in spiral flow have been clearly obtained by means of discrete wavelets transform and its multiresolution analysis. The method is composed of three steps, which are the discrete wavelets transform of the particle velocity, the inverse transform to each multiresolution level, and the reduction of the irregular data resulting in extracting the regular data. The velocity data in two dimensional space can be divided from low frequency level to high frequency level because the wavelets transform is orthonormal transform. These results lead to a new idea to estimate the air velocity from the particle velocity inversely.

6 ACKNOWLEDGEMENTS

The authors are pleased to acknowledge the considerable assistance of Mr. T. Katayanagi in Nihon University. This study is supported by Hosokawa Powder Technology Foundation in Japan.

7 REFERENCES

[1]Takei,M. Ochi,M., Horii,K. and Zhao,Y., Transporting Particles without Touching Pipe Wall, *ASME FED,* FEDSM97-3629(1997)

[2]Tsuji,Y., Discrete Particle Simulation of Gas-solid Flows (From dilute to dense flows) Review, *KONA,* 11, 57 (1993)

[3] Kubo,S., Inverse Problem Related to the Mechanics and Fracture of Solids and Structures, *JSME Int. J. Ser.I,* Vol.31, No.2, pp157-166 (1988)

[4]Molet.J. et.al Wavelet Propagation and Sampling Theory, *Geophysics*, Vol.11, (1989)

[5]Li, H., Wavelet Reynolds Stress Analysis of Two-Dimensional Vortex Flow, *ASME FEDSM*97-3040 (1997)

[6]Saito,Y., Wavelet Analysis for Computational Electromagnetics, (in Japanese), *Trans. IEE of Japan,* Vol. 116A, No10, pp833-839(1996)

[7]Horii,K., 1988, *US.PAT. No.4,721,126, UK.PAT.* No.2, 180, 957.

[8]Horii,K., Using Spiral Flow for Optical Cord Passing *Mechanical Engineering - ASME*, Vol.112, No.8, pp68-69 (1990)

[9]Horii,K. et al., A Coanda Spiral Device Passing Optical Cords with Mechanical Connectors Attached through a Pipeline, *ASME FED-Vol.121, Gas-Solid Flows,* pp65-70. (1991)